Supporting Information for

The Stabilization Mechanism and Size Effect of Nonpolar-to-Polar Crystallography Facet Tailored ZnO Nano/Micro Rods via a Top-down Strategy

Xiangyang Duan,[#a] Chao Ma,[#a] Wentao Jin,[a] Xiaoman Ma,[a] Lu'an Guo,[ac] Su-Huai Wei,[d] Jinying Yu[e] and Yelong Wu[*ab]

[a.] Shaanxi Key Laboratory of Quantum Information and Quantum Optoelectronic Devices, Xi'an Jiaotong University, Xi'an, Shaanxi 710049, China.

[b.] Key Laboratory of Nonequilibrium Synthesis and Modulation of Condensed Matter (Xi'an Jiaotong University), Ministry of Education, Xi'an, Shaanxi 710049, China.

[c.] School of Physics and Astronomy, University of Birmingham, Edgbaston, Birmingham, West Midlands B15 2TT, United Kingdom.

[d.] Beijing Computational Science Research Center, Beijing 100094, China.

[e.] School of Physics, Northwest University, Xi'an, Shaanxi, 710049, China.

*

# These authors contributed equally to the work.

1. Elemental composition analysis

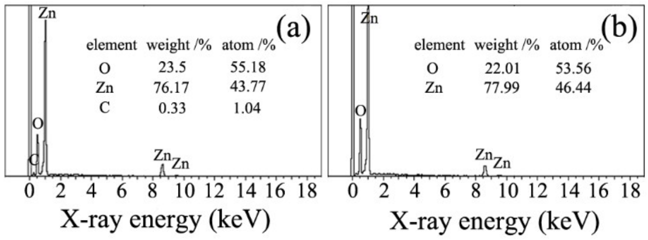

Figure S1. The corresponding EDS spectra of the as prepared hexagonal nanorods and the corrugated ones after etched.

The corresponding EDS spectra of the hexagonal nanorods and corrugated nanorods are presented in Figure S1a and S1b, respectively. The as prepared hexagonal nanorods consist of zinc, oxygen and carbon atoms, while the etched corrugated ones contain only zinc and oxygen atoms. The weight percent and atomic percent of the atoms have been marked in the images. It is intuitional that carbon atoms escape from the nanorods with oxygen atoms during the etching treatment, so the oxygen concentration also decreases in the corrugated nanorods.

2. Crystal structure analysis

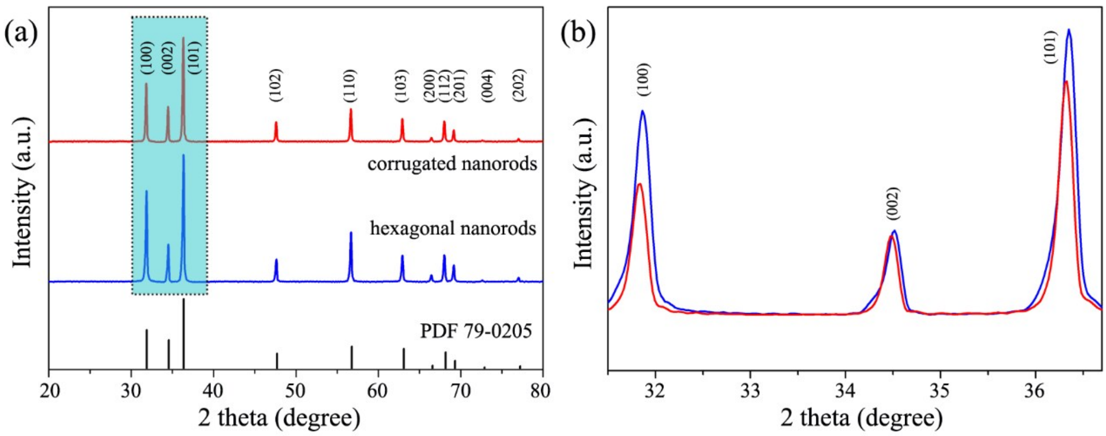

Figure S2. XRD patterns of the as prepared hexagonal nanorods and the corrugated ones after etched. (a) Full results of XRD patterns from 20° to 80° . (b) Partial enlarged image of the selected area in (a).

The XRD patterns of the hexagonal NRs and corrugated ones were also measured. Figure S2(a) presents the results from 20° to 80°. No impurity-related peaks are found in the sample, and all the diffraction peaks can be indexed as wurtzite-type ZnO compared with the standard PDF card (JCPDS, PDF 79-0205). Moreover, the diffraction angles slightly decrease after the etching treatment, see the enlarged XRD patterns in Figure S2(b). We can see that all the diffraction angles of the corrugated NRs become smaller than that of the hexagonal NRs, 31.86° to 31.82° for (100), 34.52° to 34.47° for (002) and 36.35° to 36.31° for (101). According to Bragg Equation, crystal plane spacing is inversely proportional to the sine value of corresponding diffraction angle. Therefore, we can deduce that the crystal plane spacing would decrease when the as prepared samples suffer etching treatment at high temperature, which well matches the HRTEM data in Figure 2. It is worth noting that the diffraction angles of the corrugated nanorods shift as a whole rather than anisotropic shifting, indicating that it is not a result of releasing the residual stress in the nanostructure.

3. Photoluminescence spectra analysis

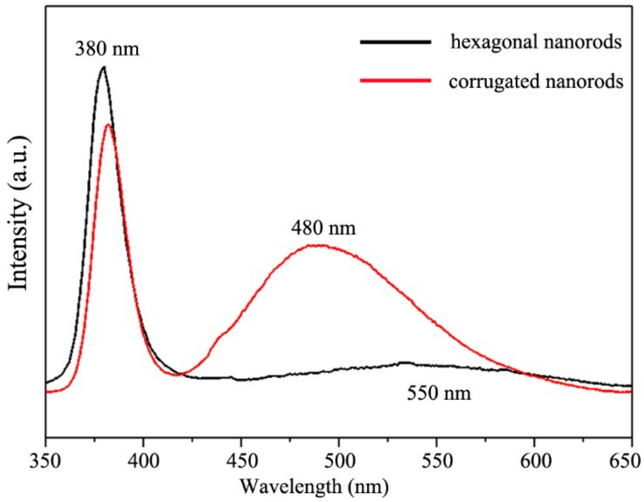

Figure S3. The PL spectra of the as prepared hexagonal nanorods and the corrugated ones after etched.

The PL spectrum has been measured to analyze the optic properties and defect types of the products, see Figure S3. The unetched sample shows two dominant emission peaks. The ultraviolet emission peak (UV peak) located at 380 nm is relative to the free exciton recombination, corresponding to the near band transition. It slightly shifts to the long wavelength area after etched, indicating that the band gap E_g decreases.[1] After the etching treatment, a broad visible emission peak appears, which can be attributed to the defects generating under elevated temperature and reductive atmosphere. It consists of at least three types of defective emission peaks, located at 400~480 nm, 520 nm and 550 nm, caused by defects of Zn_i, V_O, and OH^-, respectively.[2] Different defects emission peaks always overlap with each other and can hardly be separated. The PL spectra demonstrate that defects such as oxygen vacancy forms in the corrugated ZnO NRs. Combined with the first-principles calculation, we believed that O vacancy defect-induced reconstructions might be the reasonable explain for the forming of corrugated structure in ZnO.

References

1. X. Duan, G. Chen, P. Gao, W. Jin, X. Ma, Y. Yin, L. a. Guo, H. Ye, Y. Zhu, J. Yu and Y. Wu, Applied Surface Science, 2017, 406, 186-191.
2. Y. Li, R. Yao, H. Wang, X. Wu, J. Wu, X. Wu and W. Qin, ACS applied materials & interfaces, 2017, 9, 11711-11720.